Generation of large orbital angular momentum from superposed Bessel beams corresponding to resonant geometric modes

Y. F. Chen,* Y. C. Lin, W. Z. Zhuang, H. C. Liang, K. W. Su, and K. F. Huang
Department of Electrophysics, National Chiao Tung University, 1001 Ta Hsueh Road, Hsinchu, 30010,Taiwan
(Received 10 January 2012; published 20 April 2012)

We theoretically verify that a coherent superposition of nearly degenerate Bessel beams characterizes the family of resonant geometric modes in circular billiards. With the ray-wave correspondence, we experimentally exploit a large-aperture cylindrical waveguide to generate the resonant geometric modes with large orbital angular momentum. Furthermore, the free-space propagation of the geometric modes emerging from the cylindrical waveguide is demonstrated to display the transient dynamics of the coherent states released from a circular quantum billiard.

DOI: 10.1103/PhysRevA.85.043833 PACS number(s): 42.25.Fx, 03.65.Sq, 42.60.Da

I. INTRODUCTION

Helically phased light beams are well known to have an azimuthal phase form of $\exp(im\phi)$ and carry an orbital angular momentum (OAM) of $m\hbar$ per photon, where m is an integer [1,2]. The OAM or optical vortex of light has been exploited in a variety of applications, such as trapping [3,4] and rotating [5] of micron and submicron objects in hydrodynamics and biology, stellar coronagraphy [6], image processing [7], quantum cryptography [8], phase contrast microscopy [9], and spiral interferometry [10]. Helically phased beams with small OAM can be generated with several different techniques, such as transformation from Hermite-Gaussian modes by lens converters [11], generation from Gaussian beams by spiral phase plates [12], creation by synthesized holograms [13], generation through spatial light modulation by liquid crystal cells [14], and creation with light diffraction on dielectric wedges [15]. Nowadays, generation of light beams with huge OAM is an important and interesting task for potential applications including demonstration of optomechanical effects and trapping of cold atoms [16].

Bessel beams emerge as propagation-invariant solutions of the Helmholtz equation in a cylindrical waveguide and carry a well-defined OAM associated with their spiral wave fronts [17]. In ray dynamics, the transverse confinement of a cylindrical waveguide can be regarded as a circular billiard for light. The periodic orbits of a circular billiard can be characterized by the indices (p,q), where q is the number of turning points at the boundary during one period, and p is the number of windings during one period [18]. The average OAM of light for each periodic orbit (p,q) can be given by $\hbar(k_t R_o)$, where R_o is the shortest distance to the circular center and k_t is the transverse wave number. This indicates that it is possible to employ the geometric modes of cylindrical waveguides to generate light beams with large OAM. Even though very-high-order Bessel beams have been demonstrated using cylindrical waveguides and whispering gallery resonators [16], generation of geometric modes with huge OAM has not been realized yet. Moreover, since light interference is profoundly relevant to the underlying ray dynamics [19–21], it will be scientifically interesting to explore light beams with huge OAM from the feature of ray-wave correspondence that is analogous to the classical-quantum correspondence [22].

In this work we first explore the subtle relationship between geometric modes and high-order Bessel modes for manifesting the OAM in the ray-wave correspondence. We further develop a systematic method to generate various geometric modes with huge OAM from a large-aperture cylindrical waveguide. More importantly, we also employ the free-space propagation of the geometric modes emerging from the cylindrical waveguide to analogously emulate the transient dynamics of quantum states suddenly released from quantum billiards.

II. RELATIONSHIP BETWEEN GEOMETRIC MODES AND HIGH-ORDER BESSEL MODES

The normalized eigenstates $\psi_{m,n}(r,\phi)$ in polar coordinates for a circular billiard of radius R are given by

$$\psi_{m,n}(r,\phi) = \frac{1}{\sqrt{\pi}\,R\,J_{m-1}(k_{m,n}R)} J_m(k_{m,n}r)e^{im\phi}, \qquad (1)$$

where $m \in \mathbb{Z}$, $n \in \mathbb{N}$, and J_m is the Bessel function of the first kind and order m. The corresponding eigenvalues $k_{m,n}$ are determined by the boundary condition at the circular boundary, i.e., $J_m(k_{m,n}R) = 0$ and the quantum numbers m, n correspond to the quantization of the azimuthal and radial oscillations of the wave, respectively. In a cylindrical waveguide, $k_{m,n}$ is the transverse component of the total wave number k. For large quantum numbers, the eigenvalues $k_{m,n}$ can be determined with the Wentzel-Kramers-Brillouin (WKB) method to be given by $\sqrt{k_{m,n}^2(R^2 - R_o^2)} - m\cos^{-1}(R_o/R) = (n + 3/4)\pi$, where R_o is the distance of closest approach of the wave to the center of the billiard. The relationship between R_o and $k_{m,n}$ is given by the expression for OAM: $m\hbar = R_o(\hbar k_{m,n})$. In ray dynamics, the shortest distance to the origin R_o for the periodic orbits (p,q) is given by $R_o = R\cos(p\pi/q)$. With this expression, the quantization condition from the WKB method can be written as $k_{m,n}R\,\sin(p\pi/q) = [m(p/q) + n + (3/4)]\pi$. This quantization condition reveals that the group of the eigenstates $\psi_{m_o+q\kappa,n_o-p\kappa}$ with $\kappa \in \mathbb{Z}$ and $m_o \gg |q\kappa|$ constitutes a family of nearly degenerate states and forms an energy shell in the neighborhood of the central eigenstate ψ_{m_o,n_o}, which indicates the appearance of a sharp peak in the density of states [23].

*Email: yfchen@cc.nctu.edu.tw

In terms of the representation of the stationary coherent state [24,25], the resonant modes localized on the periodic orbits can be expressed as a coherent superposition of the eigenstates belonging to the same shell of the spectrum:

$$\Psi^{p,q}_{m_o,M}(r,\phi;\,\phi_o) = (2M+1)^{-1/2}\sum_{\kappa=-M}^{M} e^{iq\kappa\phi_o}\psi_{m_o+q\kappa,n_o-p\kappa}(r,\phi), \qquad (2)$$

where ϕ_o is related to the starting position of periodic orbits and $(2M+1)$ is the total number of Bessel modes. For a sufficiently large m_o, the larger the number M is, the more localized the resonant mode $\Psi^{p,q}_{m_o,M}(r,\phi;\,\phi_o)$ is on the orbital trajectories. It is intriguing that even for $M=1$ the resonant modes $\Psi^{p,q}_{m_o,M}(r,\phi;\,\phi_o)$ are conspicuously localized on the periodic orbits. In brief, the interference between nearly degenerate eigenmodes is extremely efficient in forming the resonant geometric modes. The efficient interference leads the resonant geometric modes to play an important role in numerous mesoscopic systems [18–22]. Figure 1 shows the numerical patterns calculated by using Eq. (2) with $M=3$ and $\phi_o=0$, where the values of the order parameter m_o are 200 and 100 for the results in Figs. 1(a)–1(d) and Figs. 1(e)–1(h), respectively. Note that the chosen values for m_o, ϕ_o, and M are not particular but were selected only for clear presentation. It can be seen that the numerical patterns for the resonant geometric modes are well localized on the periodic orbits. Since the Bessel beams with the azimuthal phase term of $\exp(im\phi)$ carry OAM [16], the resonant geometric modes naturally possess considerable average OAM. The average OAM of the geometric mode $\Psi^{p,q}_{m_o,M}(r,\phi;\,\phi_o)$ can be straightforwardly verified to be $m_o\hbar$.

Although the numerical patterns of resonant modes $\Psi^{p,q}_{m_o,M}(r,\phi;\,\phi_o)$ are clearly concentrated on the periodic orbits, it is pedagogically useful and important to explore the ray-wave correspondence in an explicit way. Next, we use the properties of the Bessel function to construct the relationship between the Bessel beams and geometric modes. Using the boundary condition $J_m(k_{m,n}R)=0$ and the asymptotic form of the Bessel function, $J_m(z)\approx\sqrt{(2/\pi z)}\cos[z-(2m+1)\pi/4]$ for $z\to\infty$, we can obtain $J_{m-1}(k_{m,n}R)\approx\sqrt{2/(\pi k_{m,n}R)}$ for the large indices. With this result and the Bessel's integral representation, the high-order Bessel modes $\psi_{m,n}(r,\phi)$ can be expressed as

$$\psi_{m,n}(r,\phi)=\sqrt{\frac{k_{m,n}}{2R}}\frac{1}{2\pi}\int_{-\pi}^{\pi} e^{ik_{m,n}r\sin\varphi}e^{im(\phi-\varphi)}d\varphi. \qquad (3)$$

In substitution of Eq. (3) into Eq. (2), the resonant modes $\Psi^{p,q}_{m_o,M}(r,\phi;\,\phi_o)$ are given by

$$\Psi^{p,q}_{m_o,M}(r,\phi;\,\phi_o)=\sqrt{\frac{k_{m_o,n_o}}{(2M+1)R}}\frac{1}{2\sqrt{2}\pi}\times\int_{-\pi}^{\pi} e^{ik_{m_on_o}r\sin\varphi}e^{-im_o(\varphi-\phi)}\times\sum_{\kappa=-M}^{M} e^{-iq\kappa(\varphi-\phi-\phi_o)}d\varphi. \qquad (4)$$

Changing the integration variable from φ to α with $\varphi-\phi-\phi_o=\alpha$ and resetting the integration bounds on the circle angle, Eq. (4) can be written

$$\Psi^{p,q}_{m_o,M}(r,\phi;\,\phi_o)=\sqrt{\frac{(2M+1)k_{m_o,n_o}}{2R}}\frac{e^{-im_o\phi_o}}{2\pi}\times\int_{-\pi}^{\pi} e^{ik_{m_o,n_o}r\sin(\alpha+\phi+\phi_o)}e^{-im_o\alpha}D_M(q\alpha)d\alpha, \qquad (5)$$

where $D_M(q\alpha)=(2M+1)^{-1}\sum_{\kappa=-M}^{M}e^{-i\kappa q\alpha}$ is the Dirichlet kernel. Since $D_M(q\alpha)$ is a periodic pulse function with period $2\pi/q$, the integration of Eq. (5) on the circle angle can be divided into q segments with the integration interval between $-\pi/q$ and π/q. Hence Eq. (5) can be written

$$\Psi^{p,q}_{m_o,M}(r,\phi;\,\phi_o)=\sqrt{\frac{(2M+1)k_{m_o,n_o}}{2R}}\frac{e^{-im_o\phi_o}}{2\pi}\sum_{s=0}^{q-1}\left\{\int_{-\frac{\pi}{q}}^{\frac{\pi}{q}} e^{ik_{m_o,n_o}r\sin\left(\alpha+\phi+\phi_o-\frac{2\pi s}{q}\right)}e^{-im_o\left(\alpha-\frac{2\pi s}{q}\right)}D_M(q\alpha)d\alpha\right\}. \qquad (6)$$

For $(2M+1)q\gg 1$, the Dirichlet kernel $D_M(q\alpha)$ displays a narrow peak concentrated in a small region of $-\Delta\leqslant\alpha\leqslant\Delta$, where $\Delta=\pi/[q(2M+1)]$. Since the effective integral range of α in Eq. (6) is rather limited, the factor $\sin[\alpha+\theta+\theta_o-(2\pi s/q)]$ for small α can be reasonably approximated as $\alpha\cdot\cos[\theta+\theta_o-(2\pi s/q)]+\sin[\theta+\theta_o-(2\pi s/q)]$. To obtain a close form, we also approximate the function $D_M(q\alpha)$ as a gate function that is 0 outside the interval $[-\Delta,\Delta]$ and unity inside it. With these approximations and $k_{m_o,n_o}=m_o/R_o$, Eq. (6) can be analytically integrated as

$$\Psi^{p,q}_{m_o,M}(r,\phi;\,\phi_o)=\sqrt{\frac{m_o}{2RR_o}}\frac{e^{-im_o\phi_o}}{q\sqrt{(2M+1)}}\left(\sum_{s=0}^{q-1}e^{im_o\left[\frac{r}{R_o}\sin\left(\phi+\phi_o-\frac{2\pi s}{q}\right)+\frac{2\pi s}{q}\right]}\right)\mathrm{sinc}\left\{\frac{m_o}{R_o}\frac{\pi}{q(2M+1)}\left[r\cos\left(\phi+\phi_o-\frac{2\pi s}{q}\right)-R_o\right]\right\}\Bigg), \qquad (7)$$

where $\mathrm{sinc}(x)=\sin(x)/x$ is the sinc function. From the property of the sinc function, the wave function $\Psi^{p,q}_{m_o,M}(r,\phi;\,\phi_o)$ can be manifestly deduced to be concentrated on the set of straight lines: $r\cos[\phi+\phi_o-(2\pi s/q)]=R_o$ with $s=0,1,\ldots,q-1$ that coincide with the periodic orbit in a circular billiard.

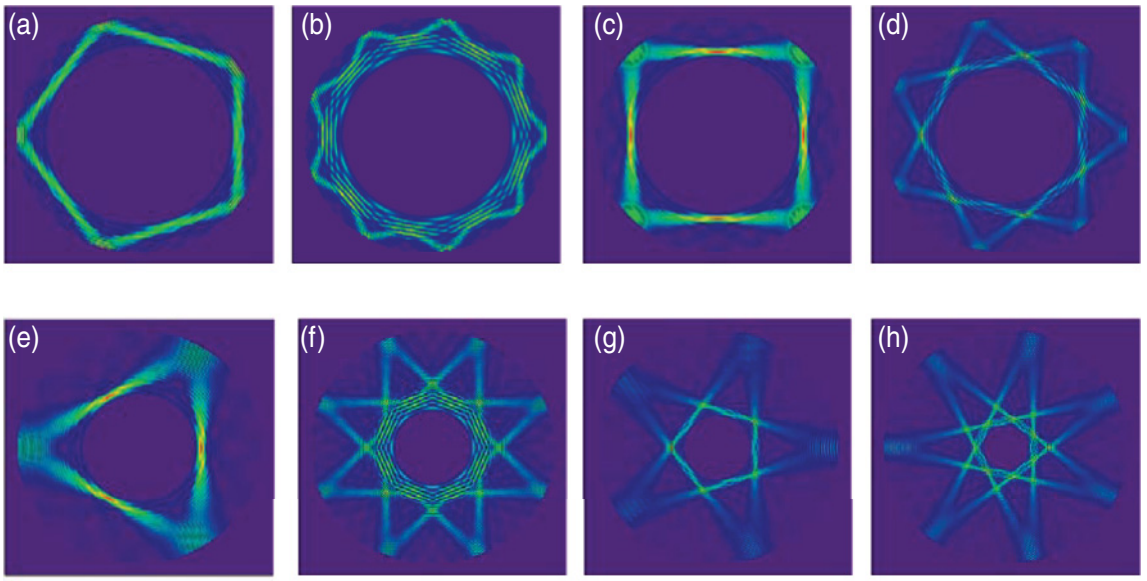

FIG. 1. (Color online) Numerically calculated patterns with Eq. (2) using $M = 3$ and $\theta_o = 0$. The values of the order parameter m_o are 200 and 100 for the results in (a)–(d) and (e)–(h), respectively.

III. EXPERIMENTAL RESULTS AND DISCUSSIONS

Cylindrical waveguides and whispering gallery resonators have been employed to generate very-high-order Bessel beams [16]. Here we exploit a large-aperture cylindrical waveguide with the precise coupling scheme to systematically generate resonant geometric modes with large OAM. Figure 2(a) depicts the experimental setup. A linearly polarized Gaussian laser beam of wavelength at 532 nm was used as an incident light source. A beam expander was employed to reduce the beam divergence less than 0.1 mrad. A lens with a focal length of 25 mm was used to focus the laser beam into the cylindrical waveguide. Figure 2(b) depicts the central angle of incidence θ_o and the effective spreading range $\Delta\theta$ in the longitudinal section of the cylindrical waveguide. The transverse path length of a ray with the angle of incidence θ_o through the waveguide is given by $L_T = L \tan\theta_o$, where L is the length of the waveguide. For the angle bandwidth $\Delta\theta$, the range of the transverse path length can be found to be $\Delta L_T = (L \sec^2\theta_o)\Delta\theta$. To form a complete transverse orbit

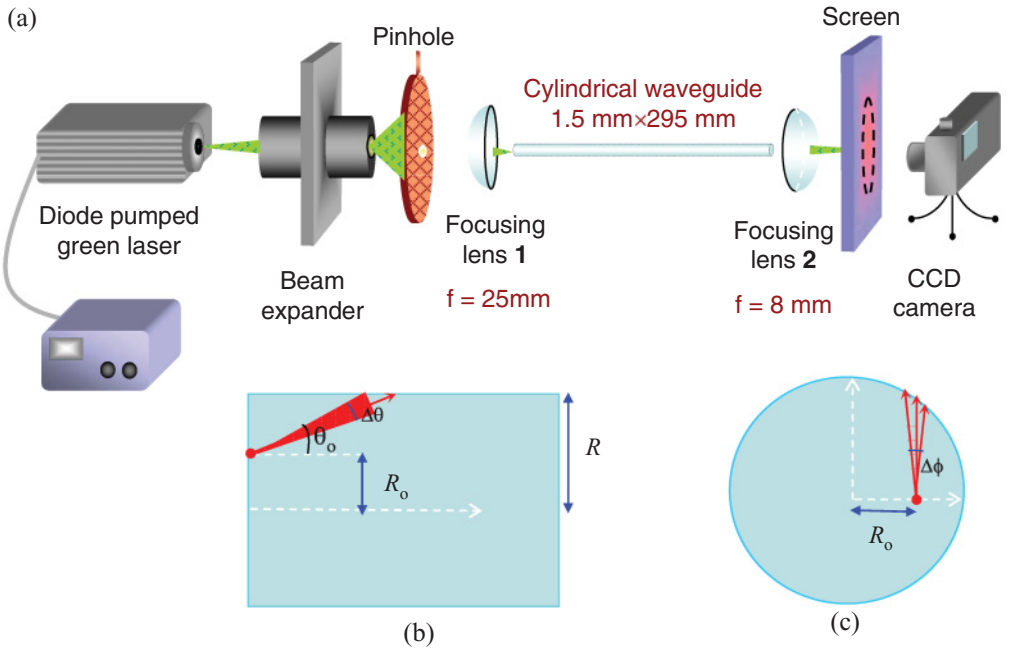

FIG. 2. (Color online) (a) Experimental setup for generating the resonant geometric modes from a cylindrical waveguide; (b) longitudinal section of the cylindrical waveguide, showing the central angle of incidence θ_o and the effective spreading range $\Delta\theta$; (c) transverse section, showing the off-axis distance R_o of the incident beam and the effective azimuthal spreading $\Delta\phi$.

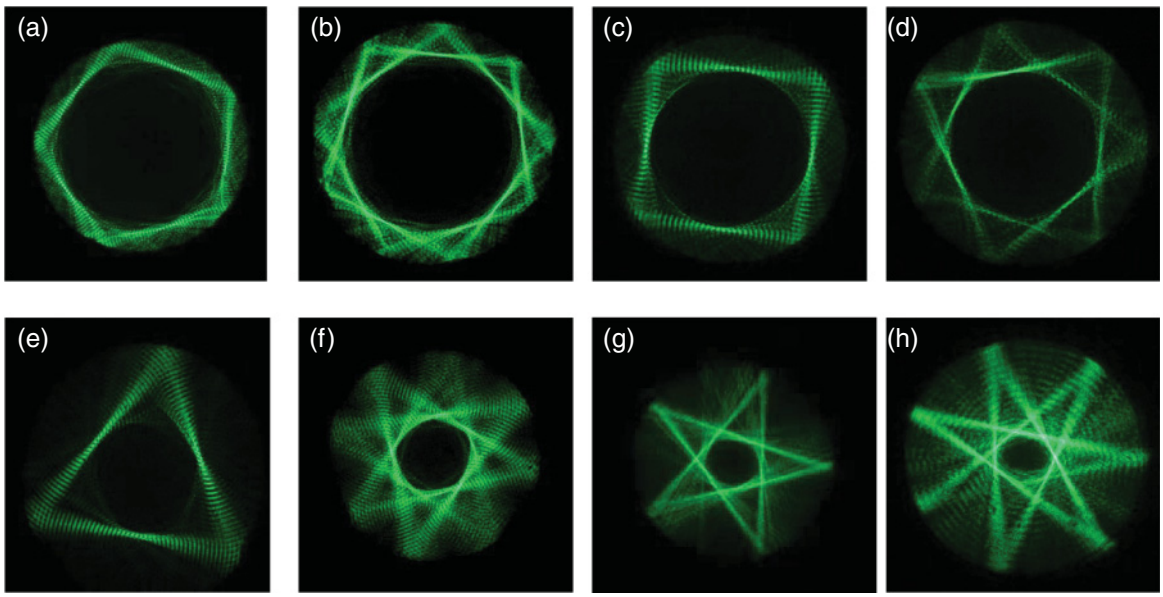

FIG. 3. (Color online) Experimental transverse near-field patterns for the observed geometric modes corresponding to the numerical patterns shown in Fig. 1.

(p,q), the range ΔL_T needs to be greater than the orbital length $L_{p,q} = 2qR\sin(p\pi/q)$. Namely, the geometric condition is given by $(\sec^2\theta_o)\Delta\theta \geqslant 2q(R/L)\sin(p\pi/q)$. A smaller aspect ratio R/L can lead to the formation of geometric modes with smaller angle bandwidth. Here we use the cylindrical waveguide with $R = 0.75$ mm and $L = 295$ mm. Figure 2(c) depicts the off-axis distance R_o of the incident beam and the effective azimuthal spreading $\Delta\phi$ in the transverse section of the cylindrical waveguide. A movable pinhole with an adjustable diameter was placed behind the beam expander to control the incident angle θ_o and the off-axis distance R_o of the laser beam. The pinhole diameter was adjusted to obtain the desired bandwidth $\Delta\theta$ and $\Delta\phi$.

We experimentally confirmed that the geometric mode with index (p,q) can be completely generated when the off-axis distance R_o is close to the value of $R\cos(p\pi/q)$. The transverse near-field pattern at the output facet of the cylindrical waveguide was projected on a screen and was imaged by a CCD camera. We controlled the incident angle to be approximately $\theta_o = 10^\circ$ and changed the off-axis distance R_o to generate various geometric modes with indices (p,q) corresponding to the theoretical results shown in Fig. 1. Figure 3 shows the near-field patterns for observed geometric modes. The experimental patterns are in good agreement with the numerical patterns showing in Fig. 1. With $\theta_o = 10^\circ$ and R_o for different geometric modes with indices (p,q), the average OAM can be calculated as $\langle m\rangle = k\tan(\theta_o)R\cos(p\pi/q)$, where k is the wave number of the incident beam. Consequently, it can be found that the average OAM ranges from $348\hbar$ to $1264\hbar$.

Another extended intriguing topic is to investigate the free-space propagation of the geometric mode because it can be analogous to the time evolution of a suddenly released two-dimensional (2D) quantum billiard wave. The optical wave

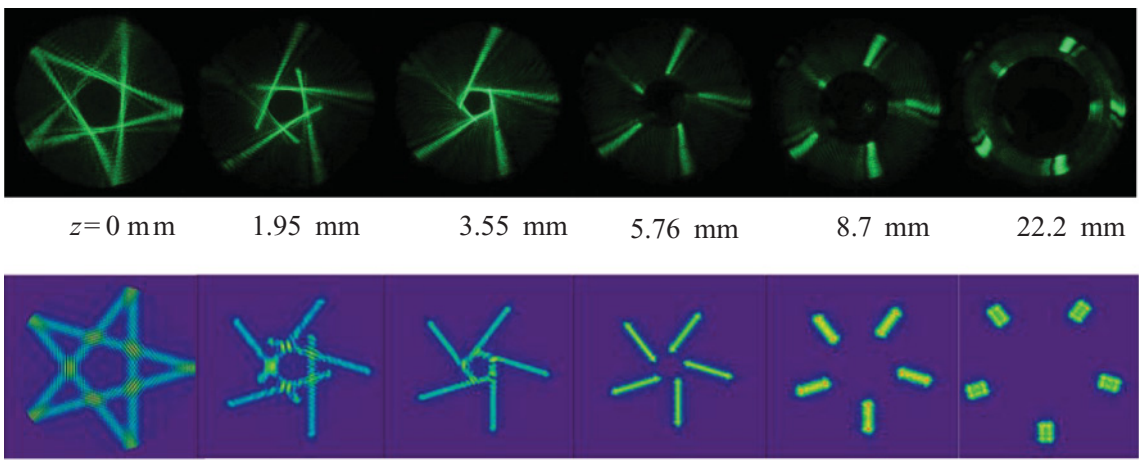

FIG. 4. (Color online) Experimental (upper row) and numerical (lower row) patterns for the quasiscarred optical modes for the case of $(p,q) = (2, 5)$ in the free-space propagation.

$\psi(x,y)$ that emerges from the output end of the light pipe at $z = 0$ to the free space in the direction of the $+z$ axis can be described with the Fresnel transformation:

$$\psi(x,y,z) = \frac{ie^{-ikz}}{\lambda z}\int dy' \int dx' \times \exp\left\{-\frac{ik}{2}\frac{[(x-x')^2+(y-y')^2]}{z}\right\}\psi(x',y'). \tag{8}$$

In quantum mechanics, the free time evolution of the quantum state $\psi(x,y)$ suddenly released at time $t = 0$ can be expressed in terms of the 2D free propagator [26,27]:

$$\psi(x,y,t) = \frac{m}{2\pi i\hbar t}\int dy' \int dx' \times \exp\left\{\frac{im}{2\hbar}\frac{[(x-x')^2+(y-y')^2]}{t}\right\}\psi(x',y'). \tag{9}$$

Comparing Eqs. (8) and (9) it is evident that the time evolution of a 2D quantum state is equivalent to the Fresnel transformation of a near-field optical wave with the substitution of $t \to z$ and $m/\hbar \to 2\pi/\lambda$, where λ is the optical wavelength. Figure 4 illustrates the experimental (upper row) and numerical (lower row) patterns for the geometric modes $\Psi^{p,q}_{m_o,M}(r,\phi;\phi_o)$ for the case of $(p,q) = (2,5)$ in the free-space propagation. Numerical patterns can be clearly seen to agree very well with experimental results. It is also worth noting that the free-space propagation of the geometric mode displays not only the feature of ray streamlines but also the spiral characteristics. The spiral feature confirms the existence of OAM that comes from the traveling-wave nature of the geometric modes in the azimuthal axis.

Finally, it is worthwhile to mention the intrinsic and extrinsic nature of the OAM in the Bessel-related geometric modes. The spin angular momentum (SAM) is well known to be independent of the reference axis and so is identified to be intrinsic. Like the OAM in the Laguerre-Gaussian (LG) beam [28], the Bessel-related geometric mode outgoing from the waveguide without passing through apertures has zero transverse momentum and may therefore be described as intrinsic. When the geometric mode propagates through an off-axis aperture to have nonzero transverse momentum, the OAM depends on the reference axis of calculation and exhibits to be extrinsic. The OAM properties of the Bessel-related geometric modes are generally the same as the LG beams with a distinct character between intrinsic and extrinsic, so-called quasi-intrinsic [29]. Recently, there have been reports on methods of converting SAM into high values of the intrinsic OAM by means of an inhomogeneous anisotropic optical element called q plate [30,31]. The q-plate element can also be employed to perform the OAM state tomography for characterizing the intrinsic and extrinsic nature [32,33].

IV. CONCLUSIONS

In conclusion, we have exploited the Bessel's integral to analytically manifest the ray-wave correspondence between high-order Bessel beams and geometric modes in circular billiards. We also experimentally demonstrated that the Bessel-related geometric modes can be strikingly generated by utilizing a large-aperture cylindrical waveguide and controlling the extent of the incident angle. Moreover, we demonstrated that the free-space propagation of the output beam emerging from the cylindrical waveguide could be used to investigate the transient dynamics of the geometric modes. We believe that the present investigation can provide important insight into quantum physics and wave optics.

ACKNOWLEDGMENTS

The authors acknowledge the National Science Council of Taiwan for their financial support of this research under Contract No. NSC-100-2628-M-009-001-MY3.

[1] J. F. Nye and M. V. Berry, Proc. R Soc. London, Ser. A **336**, 165 (1974).
[2] M. S. Soskin and M. V. Vasnetsov, Prog. Opt. **42**, 219 (2001).
[3] K. T. Gahagan and G. A. Swartzlander Jr., Opt. Lett. **21**, 827 (1996).
[4] M. Dienerowitz, M. Mazilu, P. J. Reece, T. F. Krauss, and K. Dholakia, Opt. Express **16**, 4991 (2008).
[5] J. M. Macdonald, G. Spalding, and K. Dholakia, Nature **426**, 421 (2003).
[6] G. A. Swartzlander Jr., Opt. Lett. **26**, 497 (2001).
[7] K. Crabtree, J. A. Davis, and L. Moreno, Appl. Opt. **43**, 1360 (2004).
[8] J. M. Hickmann, E. J. S. Fonseca, W. C. Soares, and S. Chávez Cerda, Phys. Rev. Lett. **105**, 053904 (2010).
[9] S. Fürhapter, A. Jesacher, S. Bernet, and M. R. Marte, Opt. Express **13**, 689 (2005).
[10] A. Jesacher, S. Fürhapter, S. Bernet, and M. R. Marte, J. Opt. Soc. Am. A **23**, 1400 (2006).
[11] E. Abramochkin and V. Volostnikov, Opt. Commun. **83**, 123 (1991).
[12] M. W. Beijersbergen, R. P. C. Coerwinkel, M. Kristensen, and J. P. Woerdman, Opt. Commun. **112**, 321 (1994).
[13] V. Yu. Bazhenov, M. S. Soskin, and M. V. Vasnetsov, J. Mod. Opt. **39**, 985 (1992).
[14] Y. J. Liu, X. W. Sun, D. Luo, and Z. Raszewsk, Appl. Phys. Lett. **92**, 101114 (2008).
[15] Ya. V. Izdebskaya, V. G. Shvedov, and A. V. Volyar, Opt. Lett. **30**, 2472 (2005).
[16] A. B. Matsko, A. A. Savchenkov, D. Strekalov, and L. Maleki, Phy. Rev. Lett. **95**, 143904 (2005).
[17] J. Durnin, J. J. Miceli, and J. H. Eberly, Phys. Rev. Lett. **58**, 1499 (1987).

[18] M. Brack and R. K. Bhaduri, *Semiclassical Physics* (Westview Press, Boulder, CO, 2003).
[19] J. Wiersig and M. Hentschel, Phys. Rev. Lett. **100**, 033901 (2008).
[20] C. Gmachl, F. Capasso, E. E. Narimanov, J. U. Nöckel, A. D. Stone, J. Faist, D. L. Sivco, and A. Y. Cho, Science **280**, 1556 (1998).
[21] N. B. Rex, H. E. Tureci, H. G. L. Schwefel, R. K. Chang, and A. D. Stone, Phys. Rev. Lett. **88**, 094102 (2002).
[22] I. V. Zozoulenko and K. F. Berggren, Phys. Rev. B **56**, 6931 (1997).
[23] W. A. De Heer, Rev. Mod. Phys. **65**, 611 (1993).
[24] Y. F. Chen, T. H. Lu, K. W. Su, and K. F. Huang, Phys. Rev. Lett. **96**, 213902 (2006).
[25] V. Bužek and T. Quang, J. Opt. Soc. Am. B **6**, 2447 (1989).
[26] M. Moshinsky, Phys. Rev. **88**, 625 (1952).
[27] S. Godoy, Phys. Rev. A **65**, 042111 (2002).
[28] T. O'Neil, I. MacVicar, L. Allen, and M. J. Padgett, Phys. Rev. Lett. **88**, 053601 (2002).
[29] R. Zambrini and S. M. Barnett, Phys. Rev. Lett. **96**, 113901 (2006).
[30] S. Slussarenko, A. Murauski, T. Du, V. Chigrinov, L. Marrucci, and E. Santamato, Opt. Express **19**, 4085 (2011).
[31] S. Nersisyan, N. Rabiryan, D. M. Steeves, and B. R. Kimball, Opt. Express **17**, 11926 (2009).
[32] E. Nagali, F. Sciarrino, F. De Martini, B. Piccirillo, E. Karimi, L. Marrucci, and E. Santamato, Opt. Express **17**, 18745 (2009).
[33] J. M. Amjad, H. R. Khalesifard, S. Slussarenko, E. Karimi, L. Marrucci, and E. Santamato, Appl. Phys. Lett. **99**, 011113 (2011).